

Vibrational predissociation spectra of size selected hydrazine clusters: Experiment and calculations

T. A. Beu,^{a)} U. Buck, I. Ettischer, M. Hobein, and J. G. Siebers
Max-Planck-Institut für Strömungsforschung, Bunsenstrasse 10, D-37073 Göttingen, Germany

R. J. Wheatley^{b)}
Department of Chemistry, University of Durham, Durham, DH1 3LE, England

(Received 4 October 1996; accepted 23 January 1997)

Vibrational predissociation spectra of hydrazine (N_2H_4)_n clusters have been measured from the dimer to the tetramer using a linetunable, isotopically substituted CO_2 -laser in order to fill the frequency gap between 990 and 1010 cm^{-1} . The clusters are size selected in a scattering experiment with helium atoms. The large blue shifts of the asymmetric NH_2 wag mode at 937 cm^{-1} are completely interpreted by calculations based on a recently determined systematic model potential. The gross shifts of 60 cm^{-1} for the dimer, 80 cm^{-1} for the trimer, and 110 cm^{-1} for the larger clusters are explained by the different structures: Cyclic arrangements with two hydrogen bonds per molecule for the dimer, rings with one hydrogen bond per molecule for the trimer, and three-dimensional structures for the larger ones. The peaks in the spectra are caused by characteristic vibrations to which more than one isomer contributes. © 1997 American Institute of Physics. [S0021-9606(97)01017-9]

I. INTRODUCTION

The photodissociation of weakly bound clusters has attracted much interest in recent years. In these experiments a vibrational mode of the molecular components is excited by infrared laser radiation. If the photon energy is larger than the binding energy of the cluster, the complex will typically dissociate according to the coupling of the molecular modes to the cluster motion. The observed vibrational dissociation spectra contain detailed information on the structure and on the absorption and decay dynamics. While the latter topic requires high-resolution spectroscopy in order to analyze the linewidth correctly¹ or direct time resolved studies,² the structural information can also be obtained from the line shift in low resolution experiments. This is especially valid, if the clusters investigated are selected according to their size.^{3,4} Experiments along these lines have been carried out for a number of systems using the momentum transfer in a scattering experiment with atoms for the size selection and a linetunable CO_2 laser for the excitations. The results available have been reviewed recently.⁵⁻⁹

In order to get the structural information, the experimental data have to be compared with calculations of the frequency shifts as function of the cluster size. While the calculations of the line shifts are well understood and practical methods are available, reliable predictions depend critically on the interaction potential. Systematic studies are therefore quite rare. One attempt is concentrated on methanol clusters for which aside from the CO stretch mode¹⁰⁻¹² also the OH stretch mode^{13,14} has been observed experimentally and analyzed theoretically using different potential models.^{9,15,16}

Very recently, we have derived a new potential for hydrazine clusters.¹⁷ Based on this potential model the experimental results for the asymmetric NH_2 wag mode¹⁸ which display large blue shifts up to 100 cm^{-1} were for the first time correctly predicted. Unfortunately the data were incomplete caused by missing lines of the CO_2 laser. Here we present new data by using an isotopically substituted CO_2 laser which exactly fills the gap in the data measured previously. These completed data set enables us to make a more detailed comparison with the calculations and to solve some discrepancies in the interpretation of the dimer and the pentamer.¹⁷ It proved to be necessary to include several isomers in the calculation for a complete interpretation of the data.

The paper is organized as follows. We start with a short description of the experimental setup. Then the experimental results are presented followed by the calculation of the line shifts of the three lowest energy isomers from the dimer to the hexamer. The paper closes with a discussion of the results.

II. EXPERIMENT

The experimental apparatus consists of a crossed molecular beams machine with two differentially pumped source chambers in a rectangular arrangement. Variation of the detection angle is achieved by rotating the source assembly around the scattering center with respect to the fixed detector unit. The detection is carried out by ionizing the clusters with 70 eV electrons in an electron impact ionizer. After having passed a subsequent quadrupole mass filter, the ions are detected by a secondary electron multiplier. For analyzing the beam characteristics, TOF-spectra of the intersecting beams are taken, using the pseudorandom chopping technique. The complete apparatus has thoroughly been described in Refs. 19 and 20.

^{a)}Permanent address: University "Babeş-Bolyai," Department of Theoretical Physics, 3400 Cluj-Napoca, Romania.

^{b)}Present address: Department of Chemistry, University of Nottingham, Nottingham NG7 2RD, England.

TABLE I. Beam data.

	N ₂ H ₄ in He	He
Mixture	5.8%	
Nozzle diameter (μm)	140	30
Pressure (bar)	1.5	30
Peak velocity (m/s)	1650	1765
Speed ratio	26	43

The hydrazine clusters are generated in an adiabatic expansion. Applying the seeded beams technique, a dilute mixture of 5.8% N₂H₄ in He as carrier gas is produced in a liquid reservoir kept at 324 K. Thus the equivalent N₂H₄ vapor pressure is mixed with He so that a stagnation pressure of 1.5 bar is obtained for the subsequent expansion through a sonic nozzle of 140 μm in diameter. The actual beam parameters are listed in Table I.

For size selection the clusters are then scattered from a helium beam. Under single collision conditions a momentum transfer takes place thus deflecting the lighter and hence smaller clusters into larger scattering angles than the heavier ones. A kinematic analysis reveals that a specific limiting deflection angle is assigned to each cluster size n , which decreases with growing n . For the relevant cluster sizes the respective angles together with the actual detection angles are listed in Table II. In this way the larger clusters cannot reach the detector. To exclude the smaller ones, a mass spectrometer is used. Here the fragmentation of the clusters is accounted for and the clusters of size n are detected at the protonated masses (N₂H₄) _{$n-1$} H⁺.²¹ The actual masses for the detection are also presented in Table II.

For dissociation the deflected beam interacts with the counterpropagating radiation of the cw CO₂ laser. The fraction of clusters being dissociated leaves the beam and this, in turn, leads to an attenuation of the signal at the detector which is tuned to the fixed mass m indicated above. Tuning the laser frequency provides as a result the dissociated fraction

$$P_{\text{diss}} = 1 - \exp[-\sigma(\nu)F/h\nu] \quad (1)$$

as a function of the frequency. Here, $\sigma(\nu)$ denotes the dissociation cross section, F the laser fluence, and $h\nu$ the photon energy. The measurements have been performed in the double lock-in technique by chopping the He beam as well as the cw-laser beam at half the frequency. This is how four different types of counting signals are generated, namely for the laser switched on and off and cluster beam on and off.

TABLE II. Detection mass, limiting angle, and detection angle as a function of the cluster size n .

n	m_{det} (amu)	Θ_{lim} (deg)	Θ_{det} (deg)
2	33	9.1	8.0
3	65	6.0	5.5
4	97	4.6	4.5
5	129	3.6	3.5
6	161	3.0	3.0

Recording these signals in four counters permits to obtain a background free signal and from these data to evaluate the percentage of dissociated clusters P_{diss} . This type of arrangement guarantees in combination with a continuous operation mode of nozzle and laser an optimized duty cycle as well as sufficient laser fluence which is the essential condition for the observation of effective dissociation.

If one compares the energy, which is necessary to dissociate one of the hydrazine clusters and which varies according to Fig. 5 of Ref. 17 from 20 to 40 kJ/mol, with the energy of the CO₂-laser photon of 12.5 kJ/mol two or more photons are required. In spite of this fact the measured fluence dependence is still linear¹⁸ so that Eq. (1) can be used for the data evaluation. The reason is that the rate limiting step is still determined by the one-photon excitation of the first photon as long as the decay rate in the upper state is fast or the level width is large compared with the detuning caused by the anharmonicity of the potential.⁹

For dissociation, two different types of continuous-wave CO₂ lasers have been used, both of which are homebuilt devices. One of them is a continuous flowing gas laser system with a dc discharge tube of 129 cm in length. For the resonator a curved ZnSe output coupler ($R=10$ m) with a reflectivity of 90% is used along with a curved grating with 150 lines mm. Although a maximum power of 20 W is achievable in this arrangement the average output is kept fixed between 5 and 10 W for practical usage. Combined with the low beam velocity, this results in a laser fluence of $F=22$ mJ/cm² and maximum dissociation rates of 50%. For further details of the laser system refer to Ref. 10. In the experiments performed here, the use of the 9P, 9R, 10P, and 10R ro-vibrational branch of the CO₂ molecule gives access to the frequency range from 916 to 1095 cm⁻¹ for spectroscopy. Unfortunately, the separation between the two branches leads to a frequency gap between 990 and 1010 cm⁻¹ with no intensity available.

With all the bands being shifted, this problem can be overcome by substituting the common isotope ¹²C¹⁶O₂ by ¹³C¹⁶O₂. For this purpose a sealed-off laser system is installed. The discharge tube with a length of 80 cm is sealed by ZnSe Brewster windows and has an additional gas reservoir to increase the active gas volume. The use of platinum electrodes together with a minute additive of water vapor supports the catalytical recombination of CO₂ molecules that have been dissociated during the discharge. An additional Teflon valve allows the gas mixture to be changed after some 1000 h of operation. The addition of a few percent of xenon leads to a cooling effect for the mixture which is normally provided by the gas flow itself. The achievable average output power amounts to 2 W and the maximum output is 4 W.

III. RESULTS

A. Experiment

The photodissociation spectra have been measured with the new laser in the frequency range from 990 to 1010 cm⁻¹ in order to fill the gap in the data set obtained previously.¹⁸ Since the power is lower than in the former

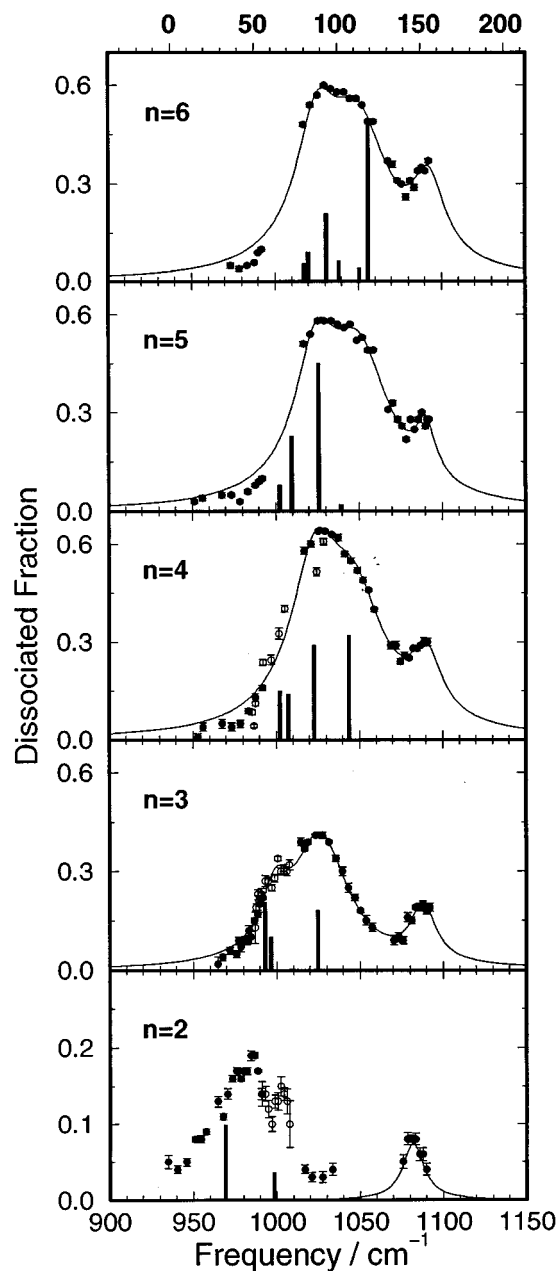


FIG. 1. Measured photodissociation spectra of hydrazine clusters (open circles: this work, full circles: Ref. 18) and calculated stick spectra based on the lowest energy configurations. The scale for the lower axis denotes the absolute frequencies, while the upper one shows the frequency shift relative to the monomer frequency of the NH_2 wag mode.

case, the same is valid for the dissociated fractions. Therefore we have normalized the new data to the previous ones at several overlapping frequencies. The results are presented in Fig. 1 as open circles together with the previous data which are displayed as full circles. The solid lines connect the measured points and are originally based on fits to Lorentzians to the complete spectrum. In case of the dimer a new peak structure appears at 1002 (64) cm^{-1} in the gap which will change the interpretation completely. The numbers in parentheses indicate the shift from the monomer value. For this shift a separate scale is given in the upper axis of Fig. 1. We

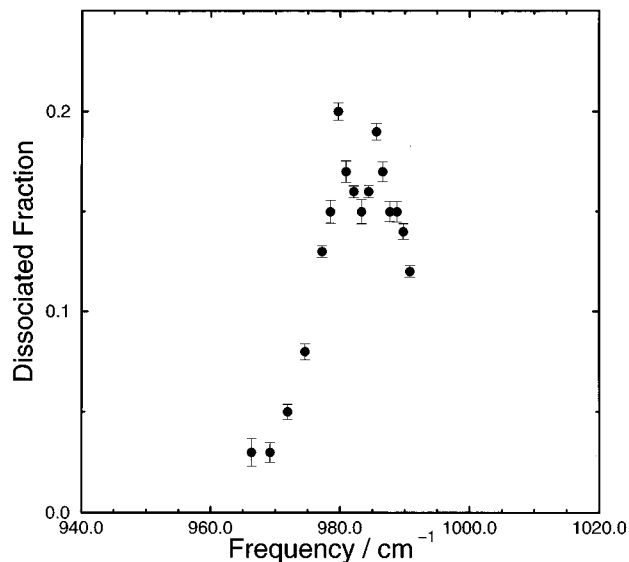


FIG. 2. Measured photodissociation spectra of cold hydrazine dimers in the direct beam.

note that there are already two less pronounced peaks present at 979 (42) and 985 (48) cm^{-1} . In order to better resolve these peaks we have repeated these measurements in the direct beam which provides much colder clusters and thus narrower lines compared with the size selected species which are slightly excited in the selection process.¹⁸ For that purpose a mixture of 0.16% N_2H_4 seeded in neon was expanded at a stagnation pressure of 2.5 bar through a 80 μm nozzle. The reservoir was kept at 264 K. If we restrict the measured frequency range to values outside the spectrum of the trimer, size selection is not necessary. The results are shown in Fig. 2. Now two very pronounced peaks are resolved at about the same positions 979.7 (42.7) and 985.6 (48.6) cm^{-1} having, however, different amplitudes.

For the trimer again a less pronounced peak is found in the gap which will change the interpretation in a qualitative way only. For the tetramer the gap is simply filled with measured points which do not change the interpretation at all. Therefore we have not measured the spectra for the two larger clusters, since the main structures are not affected. They are presented here mainly for comparison.

B. Calculations

In the following we will compare the experimental results with calculations. We concentrate here on the asymmetric NH_2 wag mode. The feature around 1080 – 1100 cm^{-1} which is attributed to the NN stretch mode is discussed in Ref. 17. For the details and the method of the calculations refer also to Ref. 17. There was demonstrated that a suitable method for calculating the IR spectra is the frozen molecule approach. It is based on perturbation theory generalized for degenerate states.^{15,22,23} The basic idea is to treat the anharmonic intramolecular force field and the intermolecular potential as a quantum mechanical perturbation of the molecular vibrations, described in the normal mode approach. For

the interaction potential, which is used to calculate the minimum energy structures and which also enters the calculation of the line shift, it turned out that only the newly developed systematic model potential was able to predict correctly the large blue shift observed for the asymmetric NH_2 wagging mode. The potential is calculated from properties of the monomers and contains the electrostatic interaction using a distributed multipole expansion and a penetration component, the repulsion, and the attractive induction and dispersion terms.²⁴

The results based on the minimum energy configurations of the different clusters are also shown in Fig. 1 as stick spectra with the calculated relative intensities. At a first glance, the predicted line shifts are in good agreement with the experiment. This is especially true for the trimer, the tetramer, and the hexamer for which only some minor problems in the intensity might exist. The general trend of the pronounced blue shift that is smallest for the dimer, the increase of this shift from the dimer to the trimer, and from the trimer to the larger clusters are correctly predicted. A closer inspection, however, reveals some discrepancies. In the case of the dimer the calculated splitting does not explain the measured splitting of about 8 cm^{-1} around 980 cm^{-1} . In case of the pentamer there are no predicted lines around 1050 cm^{-1} , where a pronounced shoulder appears in the measured spectrum.

A possible way out of this problem is that more than one isomer contributes to the measured spectra. This is clearly demonstrated by the experimental findings for the dimer which display at least three peaks. One isomer, however, can only produce two lines. Thus we have calculated the line shifts of the second and third lowest minimum energy configurations using the same potential model and the same theoretical procedure. The results are given in Table III and the calculated stick spectra are presented in Fig. 3 together with the results of the lowest energy configuration of Fig. 1. For the dimer and the trimer, the positions of the contributions of the different isomers are displayed on top of the spectra. Now the calculations are in much better agreement with the data. For the three larger clusters we get a nearly perfect prediction of the measured spectra which mainly represent the envelope of several single lines originating from the three isomers. In the case of the dimer and the trimer the lines are bunched together in two groups, in close resemblance to the measured features. There is, however, a discrepancy in the absolute shift of about 8 cm^{-1} which is, compared to the absolute value of about 60 cm^{-1} , still a small value. The different configurations which contribute to the measured spectra are given in Ref. 17 for the dimer and trimer and in Fig. 4 for the pentamer.

IV. DISCUSSION

The molecular clusters studied in this paper, $(\text{N}_2\text{H}_4)_n$, and the excited vibrational mode, the asymmetric NH_2 wag, are of special interest. We can expect a different behavior than that found for the OH stretch mode in a linear hydrogen bond that is found, e.g., in methanol clusters. First, hydrazine

TABLE III. Line shifts $\Delta\nu_{12}$ ($\nu_{12}=937 \text{ cm}^{-1}$, NH_2 wag) calculated for the second and third lowest energy configurations along with their relative intensities I_{rel} using the systematic potential for hydrazine. The binding energies E of the clusters are given in kJ/mol.

n	ν_{12}					
	E	$\Delta\nu$	I_{rel}	E	$\Delta\nu$	I_{rel}
2	-22.08	26.83	0.23	-17.56	17.22	0.03
		56.56	0.22		35.80	0.42
3	-54.42	50.20	0.32	-53.60	52.50	0.22
		60.18	0.09		61.47	0.28
		79.47	0.26		76.10	0.17
4	-91.44	57.02	0.02	-90.82	66.01	0.06
		69.48	0.24		70.74	0.42
		81.99	0.41		73.84	0.18
		100.10	0.23		101.88	0.24
5	-128.74	83.24	0.24	-128.64	68.18	0.16
		89.54	0.57		77.48	0.19
		91.28	0.12		79.03	0.08
		95.28	0.05		103.54	0.29
		122.43	0.14		117.60	0.40
6	-169.20	70.14	0.10	-168.77	58.08	0.08
		70.95	0.17		72.10	0.23
		85.69	0.44		79.83	0.38
		90.00	0.12		94.81	0.41
		100.50	0.33		95.04	0.02
		118.58	0.19		103.34	0.23

with two N atoms and four H atoms will have the possibility to form more than one donor-acceptor hydrogen bond. Second, the large amplitude motion of the four hydrogen atoms of the excited mode will experience different forces. In this respect the motion is similar to the umbrella motion of ammonia clusters.²⁵ Indeed we find large blue shifts instead of red shifts and from the beginning on more than one isomer contributes to the spectra. Let us discuss the results separately for the different cluster sizes.

In case of the "cold" dimer the measured frequencies at $979.7 (42.7)$ and $985.6 (48.6) \text{ cm}^{-1}$ are in good agreement with the previous measurements.^{7,8,18} They are also observed in Fig. 1 for the size selected internally excited clusters with shifts of 42 and 48 cm^{-1} , but with a reversed intensity. The line splitting was attributed to the nonequivalent motion of free and hindered H atoms in the dimer.^{5,7,8,18} The new results of this work add another peak at $1002 (65) \text{ cm}^{-1}$. In addition, the calculations reveal that none of the three structures found in the minimization procedure, exhibits such a small splitting. In fact the lowest energy configuration obtained with the systematic potential model exhibits line shifts of 61.4 and 32.3 cm^{-1} . This very symmetric configuration does not show any nonequivalent parts, since one hydrogen atom is hydrogen bonded and three hydrogen atoms are free in completely equivalent positions in each molecule of the dimer. The splitting is therefore caused by the collective motion of one hydrogen bonded and one free atom per molecule (61.4 cm^{-1} shift) and two free hydrogen atoms per molecule (32.3 cm^{-1} shift). Very similar results are obtained for the second lowest energy configuration which contains the same

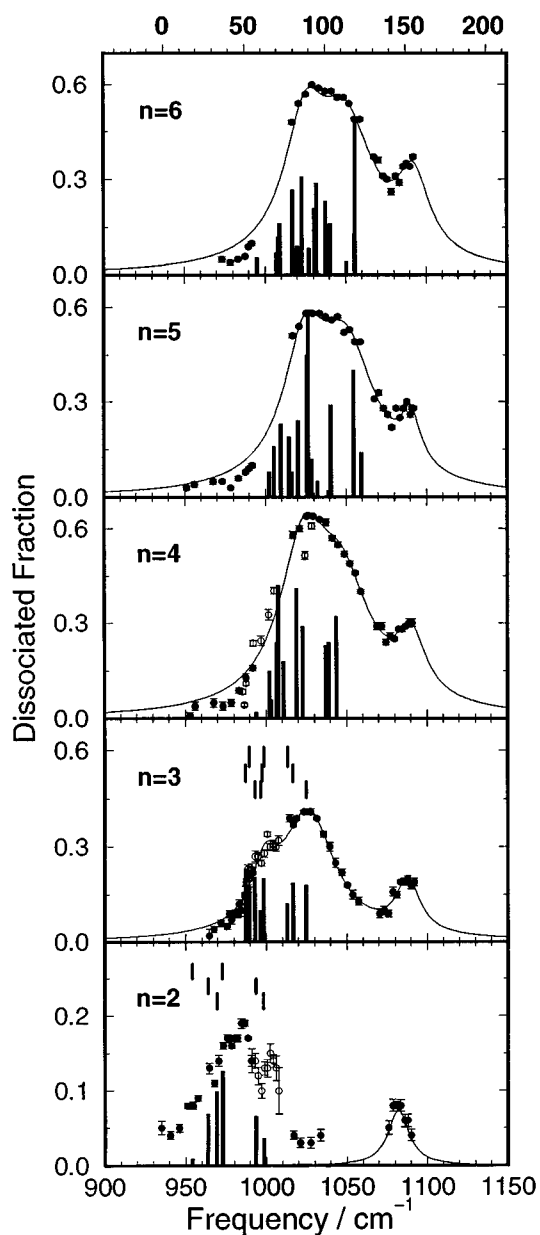


FIG. 3. Measured photodissociation spectra of hydrazine clusters (open circles: this work, full circles Ref. 18), and calculated stick spectra based on the three lowest energy configurations. For the dimer and the trimer the positions of the stick spectra of the different isomers are plotted on top of the spectra starting with those of the lowest energy configuration at the bottom. The scale for the lower axis denotes the absolute frequencies, while the upper one shows the frequency shift relative to the monomer frequency of the NH_2 wag mode.

number of bound and free H atoms in a more asymmetric way. The resulting shifts are 56.6 and 26.8 cm^{-1} . The result of the third lowest energy configuration with two hydrogen bonded H and two free H atoms in one molecule and four free H atoms in the other molecule, might be interpreted by the line shifts expected for nonequivalent positions, 35.8 cm^{-1} for the motion of the bound and 17.2 cm^{-1} for that of the free ones. The analysis shows that this picture is qualitatively true, but oversimplifies the fact that also in this case we have different combinations of free and hindered motions

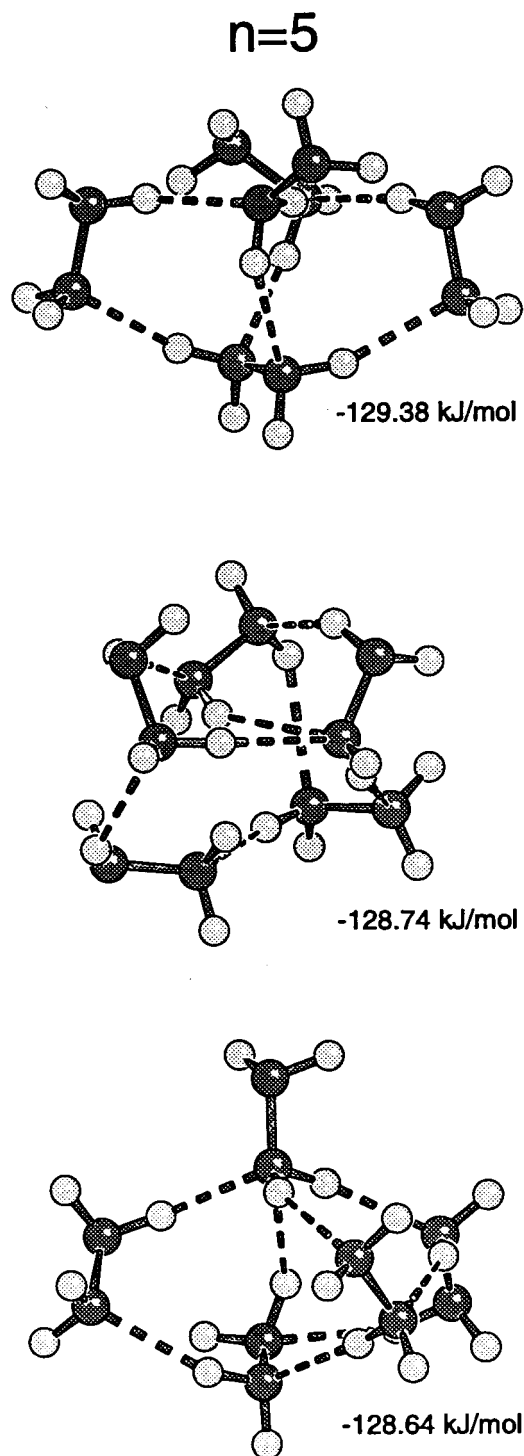


FIG. 4. The energetically three most stable hydrazine pentamer structures for the systematic potential.

which lead to the line splitting. In contrast to the lowest energy dimer, the different modes are mainly localized in only one molecule of the dimer.

Now the measured spectrum is easily interpreted. The peak at largest frequencies at 1002 cm^{-1} originates from the motion of the hydrogen bonded H atoms of the lowest and second lowest energy configuration. The next peak at 986

TABLE IV. First ($\Delta\nu_{12}^{(1)}$) and second ($\Delta\nu_{12}^{(2)}$) order contributions to the total line shifts $\Delta\nu_{12}^{\text{tot}}$ ($\nu_{12}=937\text{ cm}^{-1}$, NH_2 wag) calculated for the three lowest energy dimer configurations using the systematic potential for hydrazine. The binding energies E of the dimers are given in kJ/mol.

n	ν_{12}			$\Delta\nu^{\text{tot}}$
	E	$\Delta\nu^{(1)}$	$\Delta\nu^{(2)}$	
2	-23.99	6.74	25.55	32.29
		37.34	24.09	61.43
	-22.08	0.45	26.38	26.83
		30.72	25.83	56.56
	-17.56	4.15	13.07	17.22
		23.88	11.92	35.80

cm^{-1} is caused by the larger peak of the third lowest energy isomer and the shoulder at 977 cm^{-1} is composed by the motion of the free H atoms of the lowest two energy configurations. This interpretation also explains why the intensity of the peak at 986 cm^{-1} is larger for the warmer clusters than for the cold ones.

The calculation of the line shifts by perturbation theory allows us to trace back the origin of the line splittings to changes in certain parts of the potential. The first order contribution is essentially given by the second derivatives of the intermolecular potential [see Eq. (18) of Ref. 17], while the second order contributions come mainly from the product of the first order derivative, the force, and the intramolecular anharmonicities [see Eq. (21) of Ref. 17]. The results of this analysis for the dimers are shown in Table IV. All three isomers exhibit the same behavior. The general shifts originate from both parts, but the splitting is only caused by the first order contribution, the different curvatures, which are much larger for the hydrogen bonded parts.

The explanation for the two trimer peaks as being caused by two different isomers,^{5,8,18} one close to the dimer chain structure and one cyclic one, has proven wrong by the present calculations. First, the systematic potential exhibits only cyclic structures for the lowest energy isomers. In addition, the chain isomer does not exist anymore as stable configuration for the systematic potential model. Second, in spite of their cyclic structure, all isomers exhibit three distinct lines. Third, all three isomers contribute with one line to the largest frequency peak and with two lines to the shoulder. In general the shifts are larger than for the dimer, since now three H atoms are hydrogen bonded and 3×3 free H atoms are involved for which shifts of about 80 and $50\text{--}60\text{ cm}^{-1}$, respectively, are found. Again more than one isomer is necessary for the interpretation of the data.

This very fact is also true for the pentamer. Here the lowest energy isomer, which is rather symmetric with a total of 7 hydrogen bonds distributed in 3 single and 2 double bonds per molecule, only accounts for the first peak in the measured spectrum. Two further isomers are necessary to predict the complete spectrum. They show with a total of 8 H bonds more double (3) than single (2) bonds per molecule. This leads to the largest shift of about 120 cm^{-1} . The tet-

ramer and the hexamer spectra are already well reproduced by the 4 and 6 lines of the lowest energy isomers, respectively. The tetramer with 2 single and 2 double H bonds resembles more the symmetric pentamer, while the hexamer with 1 single and 5 double H bonds is similar to the asymmetric pentamer. Nevertheless, the contributions of the other isomers improve the picture slightly. In all cases the structures are three-dimensional so that the simple picture of cyclic structures as being the reason for the peak at 80 cm^{-1} (Refs. 5 and 18) does not hold anymore. We note, however, that the shoulder at 114 cm^{-1} which is mainly caused by molecules with two hydrogen bonds is already close to the line shift of the amorphous solid which amounts to 123 cm^{-1} (Ref. 26) and which consists probably of a three-dimensional network of molecules with two hydrogen bonds, already very similar to the structures of the hexamer. The spectrum of the crystalline solid is with 1072 and 1078 cm^{-1} (Ref. 27) out of the range of the present measurements.

In general, the agreement between theory and experiment is quite good. This is remarkable in view of the fact that the calculation of the systematic interaction potential is so to speak the first attempt and not adjusted to any experimental data. There are some deviations in the prediction of the absolute shift of the dimer and the trimer, although the structural pattern is well reproduced. Since there are no discrepancies for the larger clusters, this could be a problem of the line shift calculation, a small error in the potential, or a combination of both.

In any case the reproduction of the measured data is remarkable and we can conclude that also the cluster structures found in this analysis are quite reliable. According to the different blue shifts we find three types of structures. The dimers form cyclic arrangements with two hydrogen bonds. The trimers appear as cyclic configurations with one donor-acceptor hydrogen bond per molecule. All the larger clusters are composed by three-dimensional arrangements. In all cases more than one isomer is necessary to reproduce the data. We note, however, that these isomers are very similar in their structure.

ACKNOWLEDGMENTS

This work was supported by the Deutsche Forschungsgemeinschaft in the Schwerpunktprogramm ‘‘Molekulare Cluster’’ and the European Community by Contract SC1-CT91-0699. R.J.W. was supported by an EPSRC Research Fellowship. We thank A. Döderlein de Win for helpful assistance in the measurements with the isotopically substituted CO_2 laser.

¹R. E. Miller, *Science* **240**, 447 (1988).

²A. H. Zewail, *Science* **242**, 1645 (1988).

³U. Buck, *J. Phys. Chem.* **92**, 1023 (1988).

⁴U. Buck and H. Meyer, *J. Chem. Phys.* **84**, 4854 (1986).

⁵U. Buck, X. J. Gu, M. Hobein, C. Lauenstein, and A. Rudolph, *J. Chem. Soc. Faraday Trans.* **86**, 1923 (1990).

⁶F. Huisken, *Adv. Chem. Phys.* **81**, 63 (1991).

⁷U. Buck, *J. Phys. Chem.* **98**, 5190 (1994).

- ⁸U. Buck, in *Clusters of Atoms and Molecules*, edited by H. Haberland (Springer, Berlin, 1994), p. 396.
- ⁹U. Buck, *Adv. At. Mol. Opt. Phys.* **35**, 121 (1995).
- ¹⁰U. Buck, X. J. Gu, C. Lauenstein, and A. Rudolph, *J. Chem. Phys.* **92**, 6017 (1990).
- ¹¹F. Huisken and M. Stemmler, *Chem. Phys. Lett.* **144**, 391 (1988).
- ¹²U. Buck and M. Hobein, *Z. Phys. D* **28**, 331 (1993).
- ¹³F. Huisken and M. Stemmler, *Z. Phys. D* **24**, 277 (1992).
- ¹⁴F. Huisken, A. Kulcke, C. Laush, and J. M. Lisy, *J. Chem. Phys.* **95**, 3924 (1991).
- ¹⁵U. Buck and B. Schmidt, *J. Chem. Phys.* **98**, 9410 (1993).
- ¹⁶U. Buck, I. Ettischer, J. G. Siebers, and R. J. Wheatley (in preparation).
- ¹⁷T. Beu, U. Buck, J. G. Siebers, and R. J. Wheatley, *J. Chem. Phys.* **106**, 6795 (1996), preceding paper.
- ¹⁸U. Buck, X. J. Gu, M. Hobein, and C. Lauenstein, *Chem. Phys. Lett.* **163**, 455 (1989).
- ¹⁹J. Andres, U. Buck, F. Huisken, J. Schleusener, and F. Torello, *J. Chem. Phys.* **73**, 5620 (1980).
- ²⁰U. Buck, F. Huisken, J. Schleusener, and J. Schaefer, *J. Chem. Phys.* **72**, 1512 (1980).
- ²¹U. Buck, M. Hobein, R. Krohne, and H. Linnartz, *Z. Phys. D* **20**, 181 (1991).
- ²²T. A. Beu, *Z. Phys. D* **31**, 95 (1994).
- ²³T. A. Beu and K. Takeuchi, *J. Chem. Phys.* **103**, 6394 (1995).
- ²⁴R. J. Wheatley and S. L. Price, *Mol. Phys.* **71**, 1381 (1990).
- ²⁵F. Huisken and T. Pertsch, *Chem. Phys.* **126**, 213 (1988).
- ²⁶J. A. Roux and B. E. Wood, *J. Opt. Soc. Am.* **73**, 1181 (1983).
- ²⁷P. A. Giguère and I. D. Liu, *J. Chem. Phys.* **20**, 136 (1952).